



# Impact of boron nitride and silicon carbide on tribological properties of Al-3Gr-based hybrid composites

Serhat Şap<sup>1</sup> · Ünal Değirmenci<sup>2</sup> · Üsâme Ali Usca<sup>3</sup>

Received: 1 February 2023 / Accepted: 22 August 2023 / Published online: 11 September 2023  
© The Author(s), under exclusive licence to The Brazilian Society of Mechanical Sciences and Engineering 2023

## Abstract

In today's industry, hybrid composites based on Al-3Gr play an important role in many applications. However, improving the tribological properties and material performance is important for the widespread use of such newly developed materials in the industry. For this purpose, novel hybrid composites were produced by keeping the graphite weight (3 wt.%) in the Al main matrix and adding silicon carbide (1.5–3–6 wt.%) and boron nitride (1.5–3–6 wt.%) at different rates as reinforcement materials. Microstructural and tribological performances of hybrid composites produced by powder metallurgy method using vacuum sintering (hot pressing) were investigated. Experimental results showed that the hardness value of the matrix increased with the addition of reinforcement and that the SiC (S-2) reinforced sample had more stiffness than the BN (S-3) reinforced sample. In addition, hybrid reinforced composites were shown to have higher hardness values than single reinforced composites. The highest hardness value was recorded as 75.59 HB in sample S-6. In the wear analysis determined the lowest wear loss as  $1.34 \times 10^{-3} \text{ cm}^3$  under 1N load in sample S-6. As the applied load increases from 1 to 5 N, it was determined that the volume loss increases approximately two times, and the friction coefficient decreases about ten times. The lowest coefficient of friction was found to be 0.6746 in sample S-5. It was determined that the temperature increased 20% as the applied load increased from 1 to 5 N.

**Keywords** Al-3Gr hybrid composites · Hot press sintering · Wear · Friction

## Abbreviations

AMMC	Aluminum metal matrix composites	EDS	Energy dispersive spectrometry
P/M	Powder metallurgy	X-RD	X-Ray diffraction
HAMCs	Hybrid aluminum matrix composites	Peg400	Polyethylene glycol
MMCs	Metal matrix composites	PLC	Programmable logic controller
HAMCs	Hybrid aluminum matrix composites	ASTM	American society for testing and materials
SEM	Scanning electron microscopy	EDM	Electrical discharge machining

Technical Editor: Izabel Fernanda Machado.

- ✉ Serhat Şap  
ssap@bingol.edu.tr
- ✉ Ünal Değirmenci  
udegirmenci@bingol.edu.tr
- ✉ Üsâme Ali Usca  
ausca@bingol.edu.tr

- <sup>1</sup> Department of Electricity and Energy, Bingöl University, Bingöl, Turkey
- <sup>2</sup> Department of Machinery and Metal Technologies, Bingöl University, Bingöl, Turkey
- <sup>3</sup> Department of Mechanical Engineering, Bingöl University, Bingöl, Turkey

## 1 Introduction

Today, there is a global need for materials with low cost but high performance and acceptable quality. To meet this need, researchers started shifting away from traditional monolithic materials toward composite materials [1–6]. Conventional materials have disadvantages such as low thermal conductivity, wear resistance, hardness, weight-to-weight ratio, and corrosion resistance [7, 8]. For this reason, composite materials design aims to create more effective materials by combining the desired properties of metal and ceramic materials and eliminating the disadvantages [9–11]. But MMCs also have some disadvantages. These include high cost, difficult machinability, poor surface quality, and recycling. In

addition, more than the optimum level of ceramic particles can cause the material's brittleness and mechanical properties' deterioration. In this context, Aluminum Metal Matrix Composites (AMMC) are sophisticated engineering materials that outperform typical aluminum and alloys in terms of performance [12]. AMMCs have unique features such as high hardness, improved yield strength, a high strength-to-weight ratio, excellent thermal conductivity, a low coefficient of thermal expansion, and enhanced wear resistance [13–16]. Due to these properties, they are indispensable materials in aerospace, defense industry, automotive and various other structural applications such as airframes, pistons, transmission components, cylinder liners, bearings, brakes, propulsion oils, and submarines [17–22].

As technology progresses swiftly, turbo engines that increase efficiency by delivering combustion with small volumes and high compression ratios are gaining popularity. Therefore, hybrid reinforced AMMC structures with higher strength, high thermal conductivity coefficient and low thermal expansion values are needed in the automotive industry [23]. As an example of the studies carried out in this context, Kumarasamy et al. [24] investigated the characterization of a unique hybrid AMMC with a set quantity of fly ash cenosphere (10%) and different levels of graphite (2%, 4%, and 6%). They discovered that adding cenosphere boosted hardness and tensile strength whereas graphite decreased hardness and tensile strength. They also reported that the reinforcement particles increased the tensile strength of the aluminum matrix from 178 N/mm<sup>2</sup> to 213 N/mm<sup>2</sup>, that the addition of Cenosphere significantly increased the wear resistance, and that the wear rate was further reduced with the addition of graphite due to its self-lubricating structure. Stojanovic et al. [25] created an aluminum (Al) alloy reinforced with silicon carbide (SiC) (10%) and Gr (1–5%) and evaluated how applied stress and sliding speed affected wear behavior. The specific wear rate of Al alloy A356 including SiC (10%) and Gr (1% and 5%) reduced as the load and weight percentage of the Gr reinforcing material dropped. In another study, Nagaraj et al. [26] developed an aluminum (Al) alloy reinforced with SiC (10%) and Gr (1–5%) and studied the influence of applied stress and sliding speed on wear behavior. The specific wear rate of Al alloy A356 including SiC (10%) and Gr (1% and 5%) reduced when the load and weight percentage of the Gr reinforcing material were decreased. Ul Hag ve Anand [27] studied the friction and wear behavior of AA7075/8Si<sub>3</sub>N<sub>4</sub> composites with graphite (0–6 wt.%) additions. It was discovered that as the percentage of graphite in the base alloy increased, the microhardness and density of the composites decreased. They observed that adding graphite resulted in a linear drop in COF, although wear loss tended to reduce up to 4 wt.% graphite and then rise. Miloradović et al. [28] used the Taguchi approach to investigate the dry sliding

wear behavior of hybrid composites based on ZA27 alloy and reinforced with silicon carbide (SiC) and graphite (Gr) particles. As a result, they found that the contact load had the greatest effect on the specific wear rate, while the cutting speed had the least effect. In another study on SiC and Gr, Mosleh-Shirazi ve Akhlaghi [29] used powder metallurgy (P/M) to create Al/SiC-Gr composites with various SiC particle concentrations and 2% micron-sized graphite particles by volume. The pin-on-disk wear test method was used to study the influence of SiC content on the tribological characteristics of these hybrid composites, which were compared to their equivalents without Gr. They discovered that Al/SiC/Gr hybrid nanocomposites outperformed Al/SiC nanocomposites in terms of wear resistance. Furthermore, when SiC concentration increased, the wear rate and friction coefficient of these composites dropped. Sharma et al. [30] produced SiC + Gr (4–8%) hybrid composites with AA6082 matrix by the conventional mixing casting process. The microstructures, physical parameters such as density and porosity, and mechanical qualities such as hardness and tensile strength of the hybrid composites that were created were all examined. They discovered that hardness and ultimate tensile strength rose from 52 to 84 VHN and 163–189 MPa, respectively, while % elongation decreased from 8.6 to 5.2.

Gowrishankar et al. [31] examined the mechanical and wear characteristics of hybrid metal matrix composites in the Al6061 matrix having 5% graphite and various titanium carbide fractions. As a result, they determined that MMCs (metal matrix composites) for T6 heat treatment showed superior hardness and wear properties. Arivukkarasan et al. [32] examined the experimental examination of a composite using the stir casting process and comprising aluminum LM4 alloy as matrix and tungsten carbide (WC) as reinforcing material. They showed that increasing the presence of WC particles by weight in the LM4 matrix increased the mechanical qualities (hardness, impact strength, and tensile strength). They showed that increasing the presence of WC particles by weight in the LM4 matrix increased the mechanical qualities (hardness, impact strength, and tensile strength). Balaji et al. [33] produced hybrid composite materials by adding equal weight nano-TiO<sub>2</sub> (5%) and nano-Gr (5%) reinforcements into the aluminum matrix by powder metallurgy method and examined the wear behavior of composites. According to the results estimated by the developed mathematical model, it was reported that the measured values were quite agreeable. Sharma et al. [34] developed hybrid aluminum matrix composites (HAMCs) made of silicon carbide (SiC), and graphite (Gr) reinforced with different amounts of ceramic particles. The characteristics of hybrid composites, such as microstructure, density, and porosity, as well as mechanical qualities such as hardness and tensile strength, were investigated. As a consequence, they reported 49.5 to 85 VHN and 161.5–187 MPa for

Vickers hardness and tensile strength, respectively. In addition, they determined that the relative elongation increased from 5.3 to 8.6 as the content of ceramic particles (SiC + Gr) increased from 0 to 15% by mass. Senthil Kumar et al. [35] produced hybrid composites of A356 alloy reinforced with  $Al_2O_3$ , SiC and Gr using the squeeze casting method. The structural and mechanical characteristics of the produced composites were investigated, including density, microstructural characterization, hardness, tensile strength, yield strength, and % elongation. As a consequence, they found that the A356/3 $Al_2O_3$ -3SiC-3Gr composite had 119 BHN and 315 MPa tensile strength values. Danappa ve Swamy [36] used Al7075 as the main material in their study and strengthened the composite material by using nano-TiO<sub>2</sub> particles together with Gr microparticles. The Taguchi L<sub>9</sub> series was used to calculate the influence of wear factors on wear rate. As a consequence, they observed that the reinforcement ratio had a greater influence on wear resistance, and that wear resistance increased.

Studies indicate that hybrid MMCs can have superior properties to MMCs with a single reinforcement [20, 37–40]. In addition, AMMCs must be designed to have enhanced mechanical properties, conform to standard machining methods, and have low production costs. In this regard, the performance of composite materials depends on the choice of reinforcement materials.

As a result of the literature research, it has been determined that graphite reduces the hardness and tensile strength of the materials but improves the tribological properties. For this reason, this study it is aimed to improve the mechanical properties by taking advantage of the lubricating property of graphite and adding hard reinforcement particles. As a result, the focus of this research was on the manufacturing, tribological-mechanical characterization of a Silicon carbide (SiC) and Boron nitride (BN) reinforced Aluminum–graphite matrix composite structure. By adding SiC and BN to the aluminum matrix material, the mechanical properties of the material are improved, and the machinability of AMMC is improved by adding Gr. Within the scope of this study, while the amount of Gr added to the structure remains constant at 3%, six distinct AMMC structures were produced by adding SiC and BN at varying rates individually and in combination. With this study, a new hybrid reinforced Al-Gr matrix composite structure, which has both light and high

mechanical strength, and acceptable processing capability thanks to the Gr in the structure, will be revealed.

## 2 Experimental details

This study produced new hybrid composite materials by adding SiC and BN reinforcements to the Al-3Gr matrix obtained by improving Al powders with a constant (3%) ratio of Gr powders. In addition, the microstructure, hardness, and wear characteristics of the Al-3Gr/SiC-BN hybrid composites were investigated. Moreover, the effects of different reinforcements and reinforcement ratios on the hardness and wear parameters of the material were investigated.

### 2.1 Material composition, microstructure and fabrication

Al, Gr, SiC and BN powders to be used in the study were obtained from Nanokar (Istanbul, Turkey). Table 1 shows some physical properties of powder particles used in Al-3Gr/SiC-BN hybrid composite experiments.

Six different composite materials were produced to be used in the experiments. Table 2 shows the reinforcement ratios of the powder particles in the manufactured composite samples.

The powders, whose SEM micrographs and grain sizes are given in Fig. 1, were weighed according to the desired weight percentage. The prepared powders are first dried in an oven at 100 °C. Then, they were weighed according to

**Table 1** Properties of powders in Al-3Gr/SiC-BN hybrid composite

Powders	Al	Gr	SiC	BN
Purpose	Matrix phase	Developer additive	Reinforcement	Reinforcement
Density (g/cm <sup>3</sup> )	2.71	2.26	3.21	2.1
Melting temperature (°C)	660	3652	2830	2973
Particle size (µm)	45–75	≤44	45–70	≤10
Purity (%)	≥99.90	≥98.00	≥98.00	≥99.00

**Table 2** Reinforcement rates of 6 different composite materials produced

Samples no	Al ratio (wt.%)	Gr ratio (wt.%)	SiC ratio (wt.%)	BN ratio (wt.%)
S-1	97	3	–	–
S-2	91	3	6	–
S-3	91	3	–	6
S-4	94	3	1.5	1.5
S-5	91	3	3	3
S-6	85	3	6	6

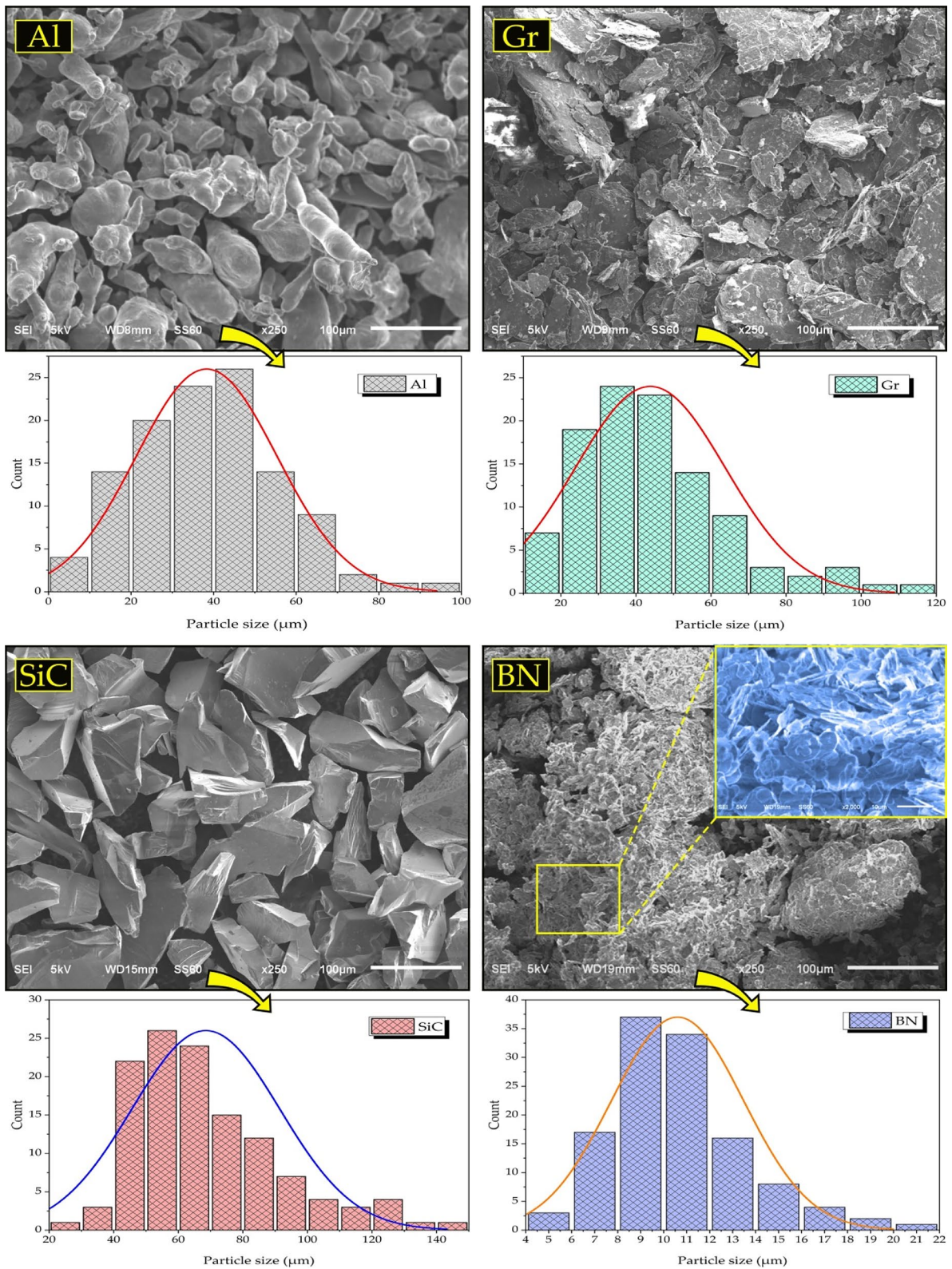


Fig. 1 SEM images and dimensional analysis graphs of raw powders

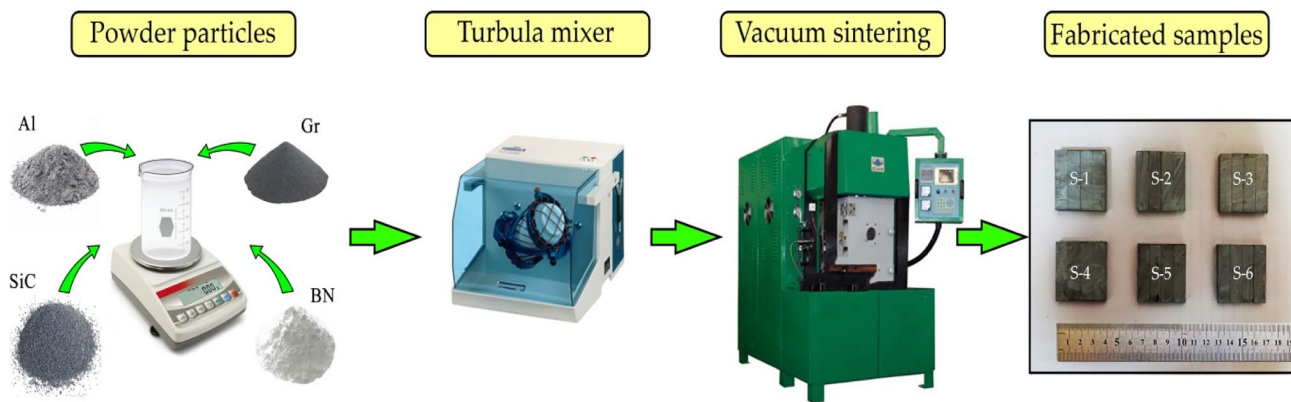


Fig. 2 Scheme showing the production processes of composites

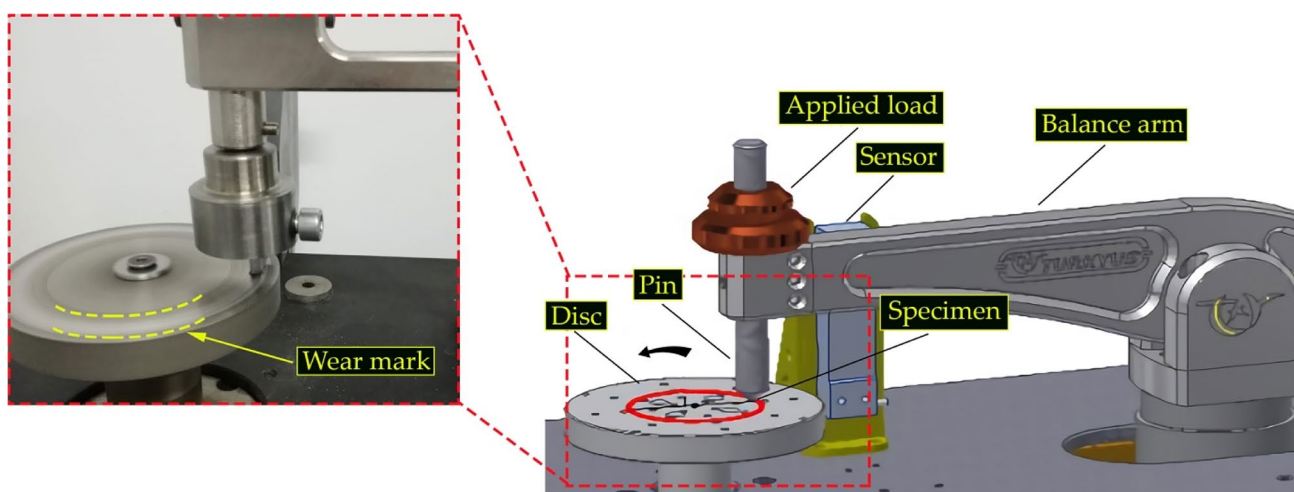


Fig. 3 Details of wear device

Table 3 Some disc attributes that were utilized in wear testing

Material	Manufacturing method	Applied process	Micro-Hardness (HV)	Surface roughness (Ra)
AISI D2 quality steel	Wire EDM	Surface hardening by nitriding	795 HV	4.6 μm

the % weight ratios given in Table 2 using a balance with  $10^{-4}$  g sensitivity and grouped separately for each composite.

Precisely weighed powders with different specific gravity and different particle sizes are mixed homogeneously using a TURBULA mixer (Cel-mak Group 7 T, Turkey). In the mixing process, 2 wt.% Peg400 (polyethylene glycol) is added together with the powders. The purpose of the added Peg400 is to prevent the powders from spilling out of the graphite mold and to obtain a homogeneous structure. Mixing is carried out using 1/3 steel balls for 150 min. The use of balls prevents agglomeration. After mixing, the powders are poured into graphite molds. Then, the powders in the mold are sintered for 10 min under a temperature of 530 °C

and a pressure of 35 MPa using a PLC (Programmable logic controller) controlled hot press machine (Zhengzhou Golden Highway, SMVB80, China). Thus, rectangular composite specimens with a length of 40 mm, a width of 40 mm and a thickness of 8 mm are produced. Oxidation formation can be observed during production. To prevent this situation, protective nitrogen gas was used. The test chart of the production above processes for composite samples is given in Fig. 2.

After the composite samples are produced without any problems, the deformed layers on the surface should be removed. In addition, it is necessary to determine the grain boundaries and examine the structure to obtain high quality

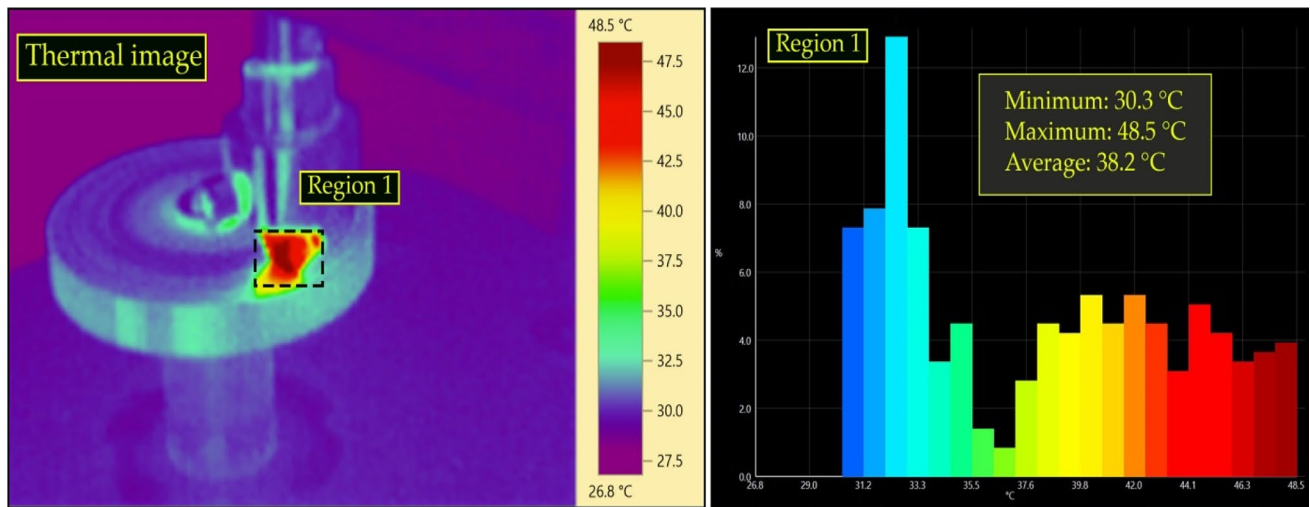
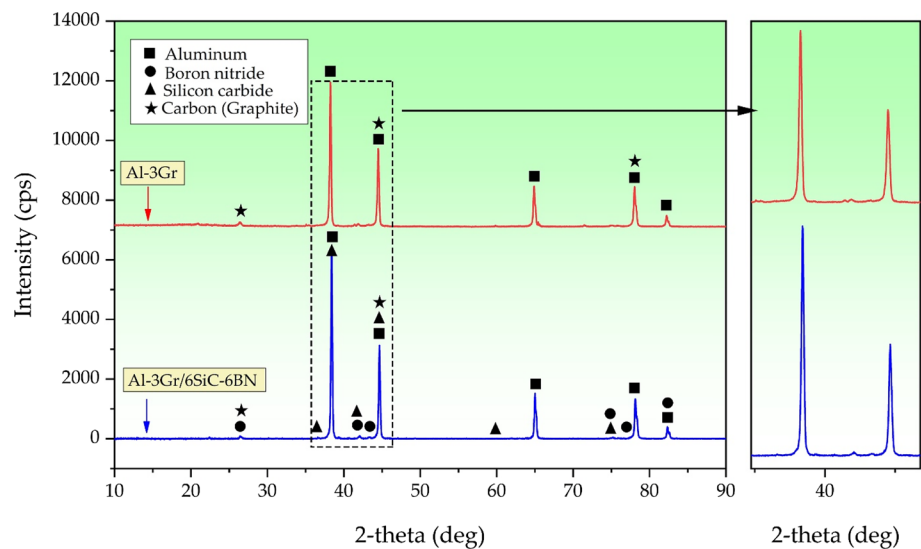


**Fig. 4** Thermal camera image and temperature distribution

**Fig. 5** X-RD analysis of S1 and S-6 sample



micrographs. Therefore, the composite samples are sanded using SiC papers, and their surfaces are clean. SiC papers varying between 200–1200 grids were used in this study. After sanding, the surfaces must be polished. One micron diamond solution was used for this polishing process. Finally, the polished surfaces must be etched. The content of the solution used is 25 ml HCl 1–2 gm  $\text{Fe}_3\text{-Cl}$ -100 ml  $\text{H}_2\text{O}$  [41]. SEM, EDS and mapping analyses were used to observe the homogeneous distribution of the reinforcement materials in the samples and determine the particle sizes. The brand of SEM used to examine microstructure and surface morphologies is JEOL JSM 6510. In addition, the "X-RD, RIGAKU ULTIMA IV" brand X-Ray Diffraction Spectrometer was used to determine the composite material's phase components and examine the crystal structure. In addition, After

the wear test, SEM analyses were done to assess the surface morphologies.

## 2.2 Density and hardness tests

To examine the physically properties of the composite materials, firstly, the density measurements of the samples were carried out. First, density measurements were made according to the Archimedes principle. Then, to increase the accuracy of the measures, they were repeated five times, and their arithmetic averages were calculated. In addition, the theoretical densities were calculated, and the relative densities were calculated over the experimental and theoretical densities [42].

Hardness measurement tests were carried out in EMCO TEST DuraJet (ZwickRoell, Austria) brand Brinell hardness

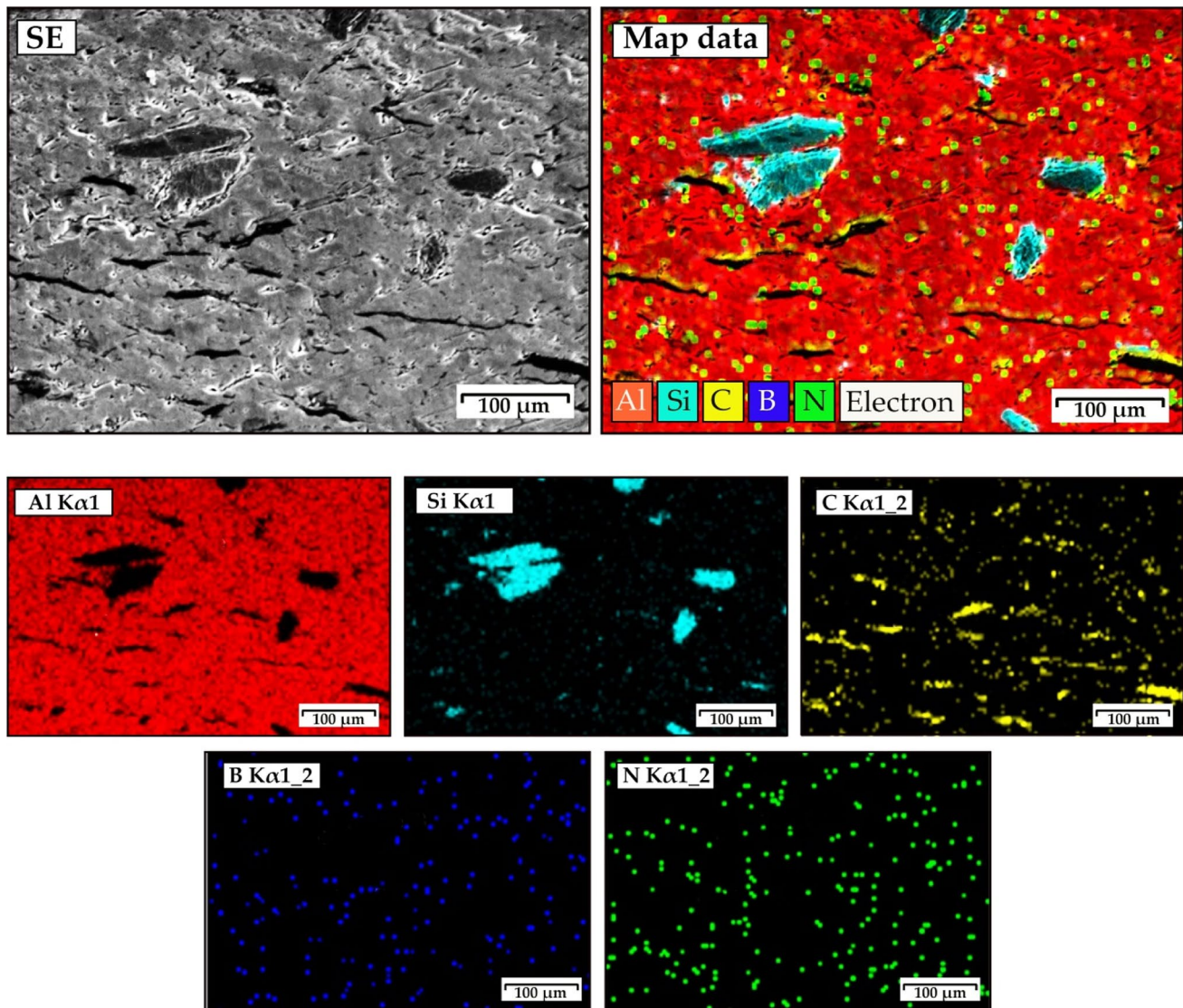


Fig. 6 SEM and elemental mapping images of sintered S-6 sample

device. Hardness measurements were made by ASTM E10-18 standards. To obtain more accurate and reliable results in hardness tests, the ball must be contacted with both the main matrix and the carbides. For this reason, macrohardness tests were preferred. Measurements were made by applying a preload of 31.25 kg to the smooth and flat surfaces of the samples for 10 s. To reduce measurement errors, five measurements are taken from each sample from different points, and the final hardness results are obtained by taking the arithmetic average of the measurements.

### 2.3 Wear characterization

Wear tests of hybrid AMMC structures were carried out with the pin-on-disc technique by ASTM G99-95a standards.

A TURKYUS (Turkyus machine, Turkey) brand tribotest device was used in the abrasion tests. Furthermore, the trials were conducted in dry sliding circumstances in a room with a temperature of 25 °C and a relative humidity of 40–50%. A total of 18 wear and friction tests were carried out. An exemplary representation of the abrasion tester is given in Fig. 3.

Some properties of the abrasive disc used in wear tests are given in Table 3. First, the abrasive disc and samples are washed and dried using high purity acetone before each experiment. The impacts of MMC type and applied load levels on composite material wear parameters such as volume loss, temperature, and coefficient of friction were then examined using wear experiments. For this reason, the sliding velocity (1.257 m/s) and the wear distance (200 m) were kept constant while the wear tests of the samples were carried out, and analyzes were carried out by choosing six

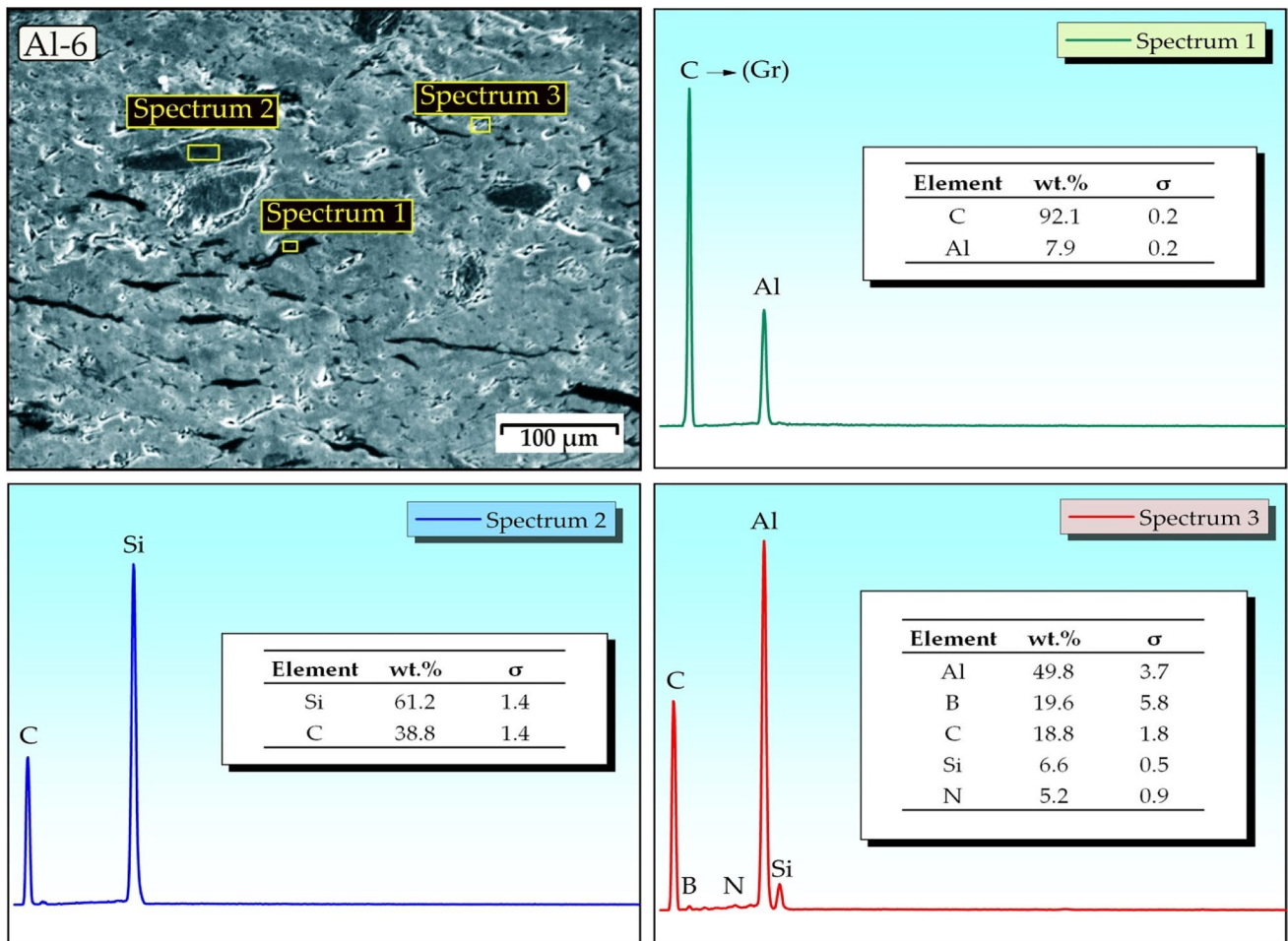


Fig. 7 EDS analyses taken from different regions of the S-6 sample

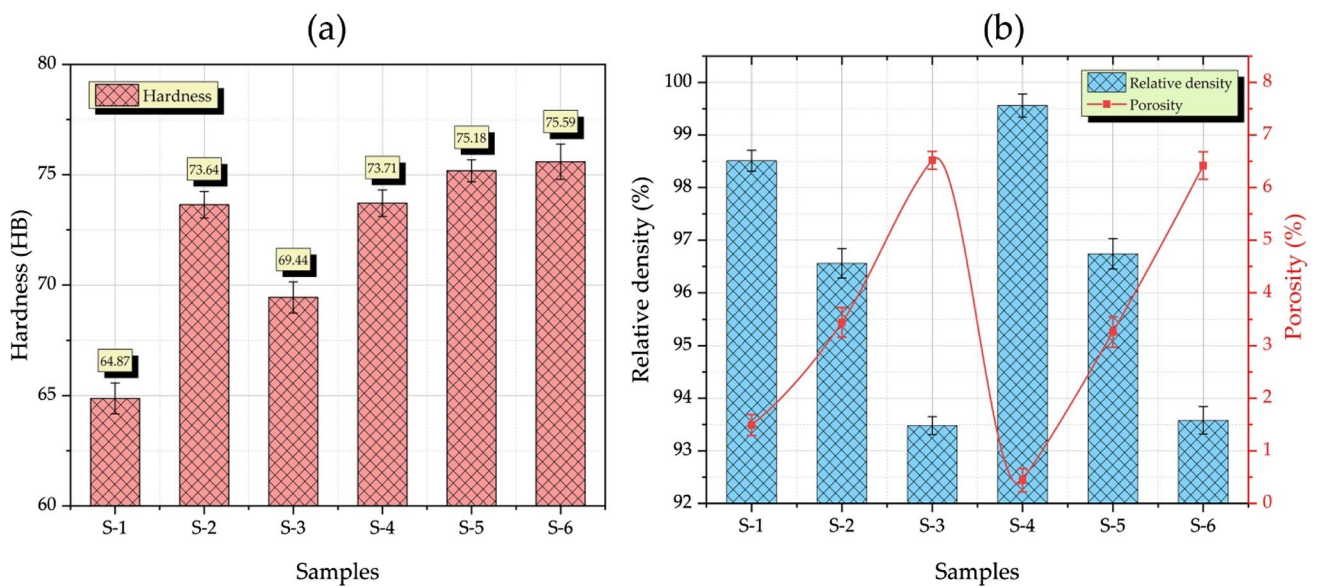
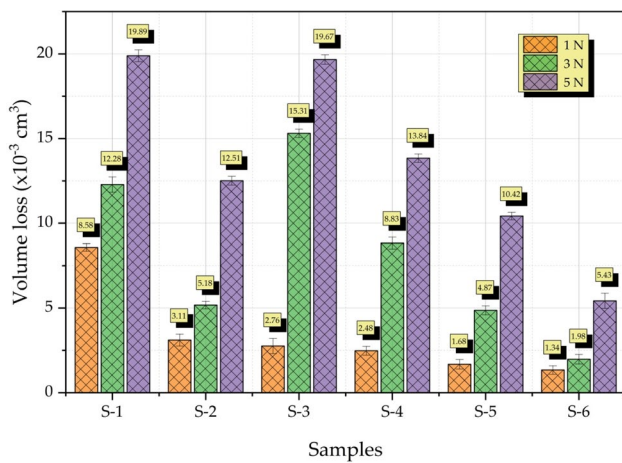


Fig. 8 Hybrid composites; **a** Hardness analysis, **b** Relative density analysis





**Fig. 9** Volume losses under different loads in the abrasion test of hybrid composites

**Table 4** Calculated wear coefficients for all samples ( $\times 10^{-6} \text{ mm}^3/\text{N.m}$ )

Sample	1 N	3 N	5 N
S1	42.92	20.46	19.89
S2	5.53	1.96	1.51
S3	76.81	4.66	40.21
S4	112.41	48.05	43.84
S5	6.72	4.79	10.42
S6	8.41	3.31	2.43

different composite structures and three additional loads (1–3–5 N) values.

Strain gauge connected to the tribo-tester used to measure friction forces during the wear test. To calculate the volume loss values, after the abrasion test, the samples were cleaned with isopropyl alcohol (IPA), and their weights were calculated. The temperature build-up between the rubbing objects during the wear test is important and needs to be examined. For this reason, temperature measurements were made using the Testo 871 (Testo SE & Co. KGaA, Germany) thermal camera. Measurements are made by taking five different temperature measurements from a fixed distance (50 cm). An example thermal image and temperature distribution graph are shown in Fig. 4.

### 3 Results and discussion

#### 3.1 Microstructural analysis

In Fig. 5, the X-RD patterns of composite no S-1 and S-6, in which all the particles are together, are seen. Analyzes were performed at  $20^\circ$  and  $90^\circ$  diffraction angles. Al diffraction peaks;  $38.33^\circ$ ,  $44.56^\circ$ ,  $64.84^\circ$ ,  $77.91^\circ$ ,  $82.09^\circ$  are confirmed with (JCPDS card no 43–13,217). Gr diffraction

peaks;  $26.84^\circ$ ,  $44.14^\circ$  (JCPDS card no 10–11060). Si diffraction peaks;  $35.09^\circ$ ,  $38.35^\circ$ ,  $60.29^\circ$ ,  $71.71^\circ$  (JCPDS card no 23–10,936). BN diffraction peaks;  $26.66^\circ$ ,  $41.69^\circ$ ,  $43.93^\circ$ ,  $71.25^\circ$ ,  $76.11^\circ$ ,  $82.31^\circ$  (JCPDS card no 90–08997). It is seen that the Al and Gr peaks are compatible with previous studies [43, 44]. The presence of Al, Gr and Si particles at high peaks were proven. In addition, BN particles were observed in small peaks.

Figure 6 displays SEM and elemental mapping analysis images of hybrid composites strengthened with SiC and BN. It is known that homogeneous mixing in composite materials is highly effective on mechanical properties. The inclusion of reinforcing particles makes the matrix strong, similar to a skeleton. The strength of the composite is dependent on the establishment of a good contact between the matrix and the particles. A good interfacial bond is possible with less porosity. With the high relative densities obtained, it can be said that the porosity is not high in the composites. From the SEM and mapping photographs taken from the surface, it is seen that there is a homogeneous distribution, and no agglomeration is observed. In powder metallurgy-produced composites, the formation of pores is inescapable [45]. Since the production of hybrid composites is made by the hot pressing method, very high densities were obtained. An increase in densities means a decrease in porosity. In general, SiC and BN particles were well bonded to the matrix as the porosity was low in all samples. In addition, since SiC particles have sharper edges and corners, they can adhere to the matrix structure more.

Figure 7 represents the EDS analysis from sample S-6, where all particles are most concentrated. As a result of the analysis, the spectrum 1 region is Gr, the spectrum 2 region is SiC and the spectrum 3 region is a region where all particles are present. Consequently, EDS analysis once again verified the particles in the hybrid composites. Figure 7 also shows the weight ratios of the components in the EDS analysis zones in tables.

#### 3.2 Hardness and density analysis

The relative density and macro-hardness of hybrid composites manufactured at different ratios are shown graphically in Fig. 8. According to the macro-hardness study, the hardness rose with the addition of reinforcing material, and the samples reinforced with SiC (S-2) had a higher hardness value than the samples reinforced with BN (S-3). Reinforcement materials in the material cause the grain sizes to be thinned and the dislocation movements to be restricted in the matrix material during the sintering process. In addition, ceramic reinforcements prevent crack propagation as load transfer occurs from matrix to ceramic reinforcements in composite materials under load [46–48]. For this reason, SiC and BN reinforcements in Al-3Gr composite are of

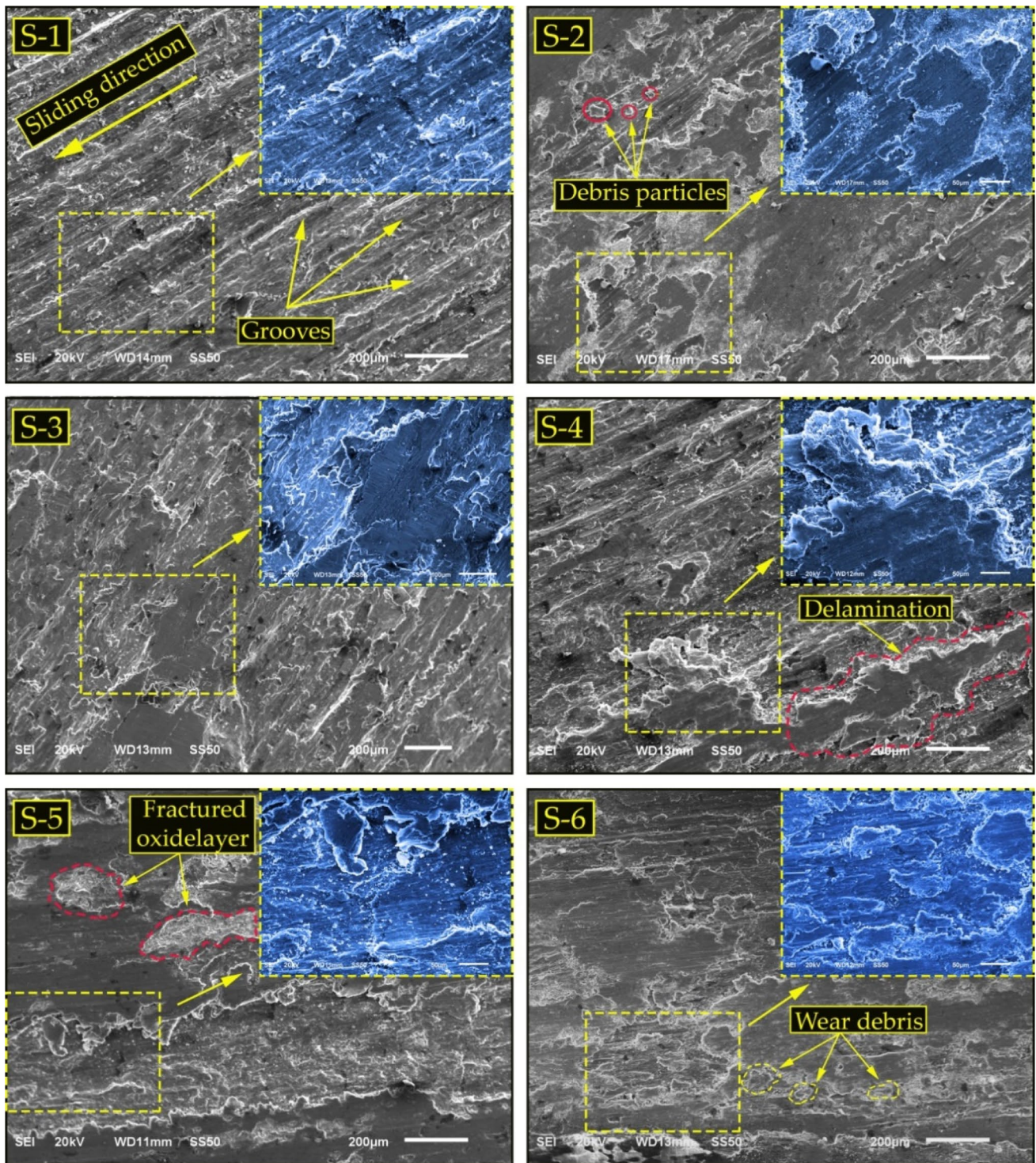


Fig. 10 Surface SEM images after wear under 5 N load

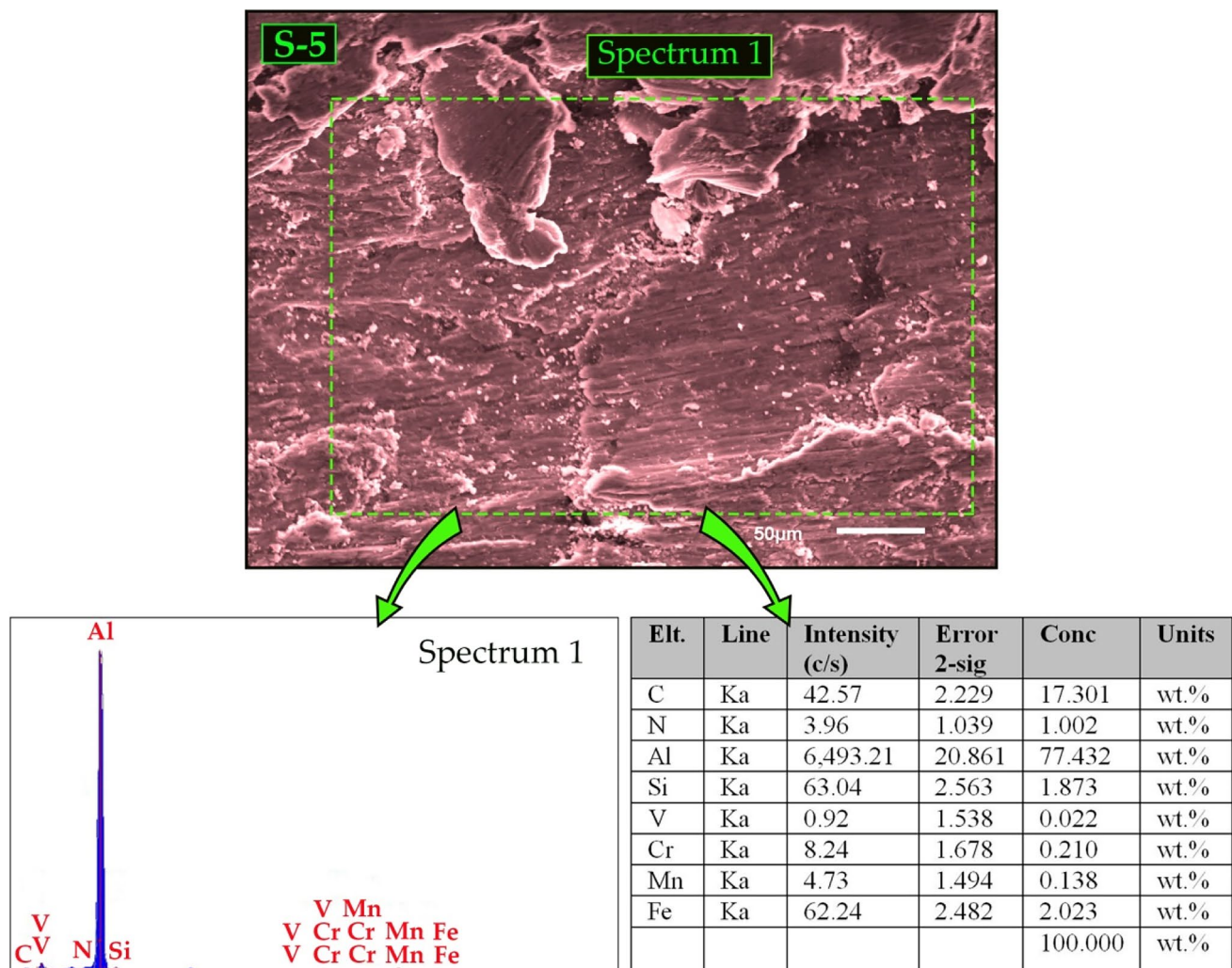


Fig. 11 EDS analysis from S-5 sample

great importance in plastic deformation. In addition, it was noted that the hardness was better in the hybrid structure with both reinforcements (SiC-BN), and the hardness values increased with the reinforcement ratio. The highest hardness (75.59 HB) was observed in the S-6 sample. The addition of hard composite reinforcement particles to the main matrix increases the structure's surface area while reducing the particulate diameters of the matrix. In addition, these hard particles transform the composite from a ductile to a brittle one and make it more resistant to plastic deformation [49]. As a result of the hard reinforcement particles, the hardness values of Al-Gr based hybrid composites rise. The increase in the reinforcement ratio decreased relative density (Fig. 8b). In the S-4 sample, the greatest relative density value was determined to be 99.56%. It can be seen that the values of hardness and relative density vary inversely proportionately.

### 3.3 Wear analysis

Figure 9 represents the volume loss graph obtained from wear analysis of hybrid composites under different loads. In Table 4, the calculated wear coefficients for all samples are given. The applied loads vary between 1 and 5 N. It is seen that the volume loss of the S-2 (Al-3Gr/6SiC) sample is reduced compared to the S-1 (Al-3Gr) sample. There is more volume loss in the S-3 (Al-3Gr/6BN) sample compared to S-2. From this point of view, it can be said that the wear performance of SiC from single reinforcements is better. It is seen that the volume losses decreased after the S-3 sample. Hard ceramic reinforcement particles improve AMMC's abrasion resistance and decrease volume loss [50]. When the studies in the literature are examined, it is seen that they are compatible with the results obtained [51, 52].

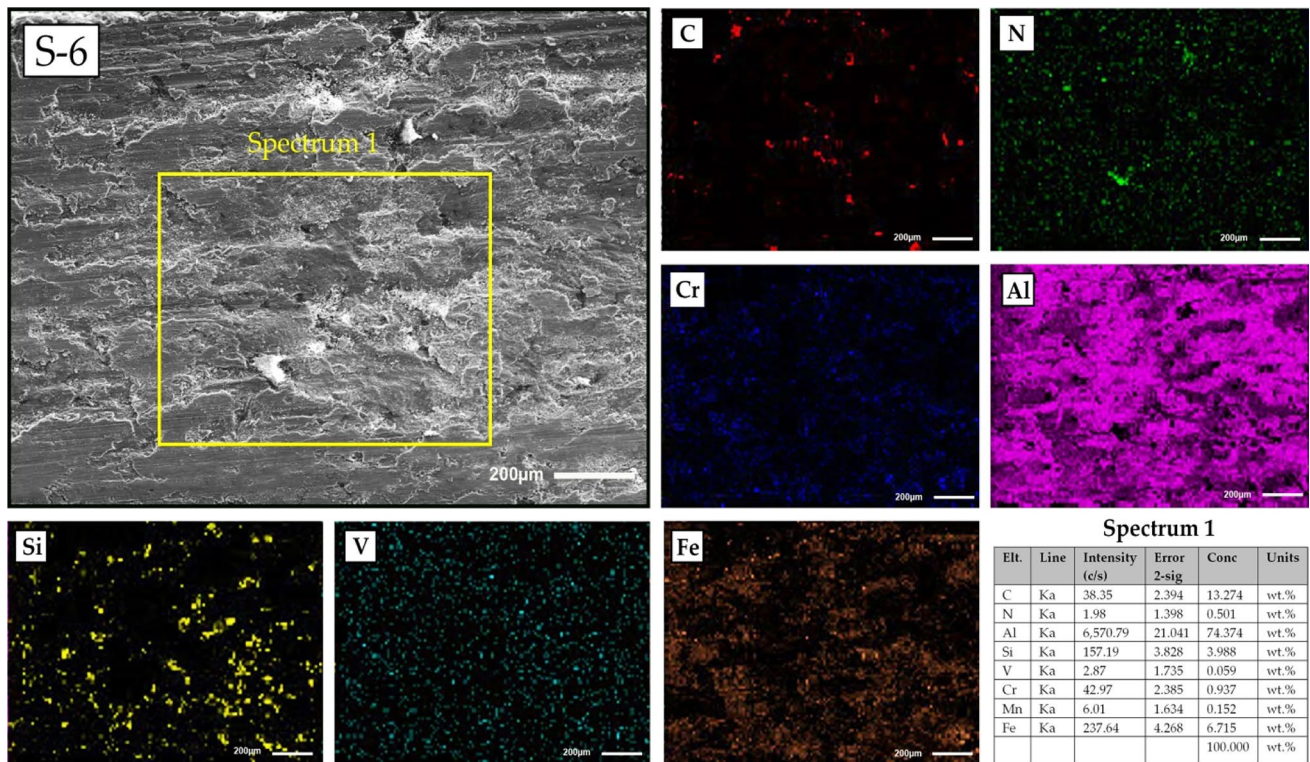
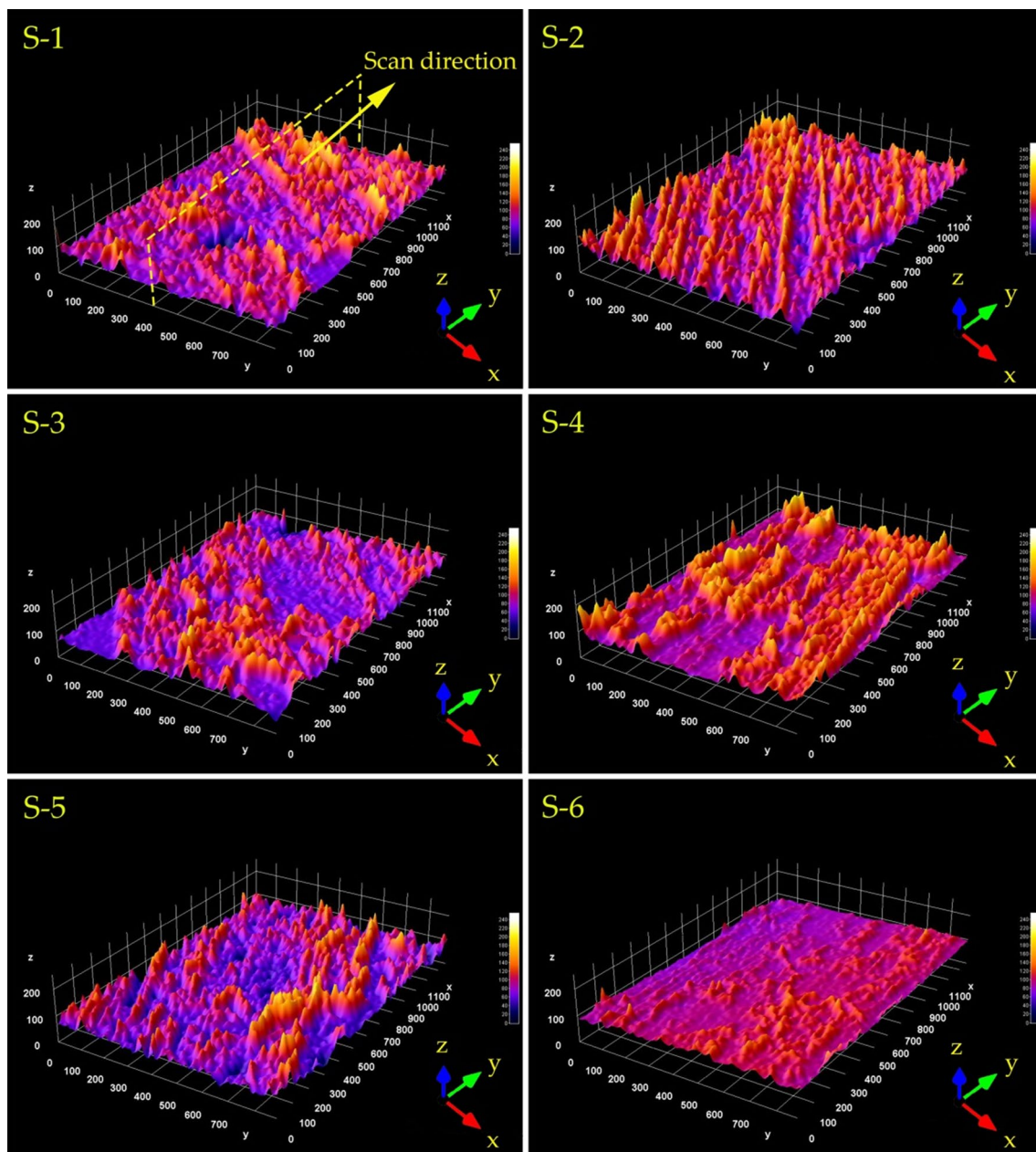


Fig. 12 Mapping analysis from the eroded surface of the S-6 sample

As the proportions of hybrid reinforcements increase, their wear performance also increases. The lowest volume loss was recorded as  $1.34 \times 10^{-3} \text{ cm}^3$  in the S-6 (Al-3Gr/6SiC-6BN) sample under 1 N load. An approximately 84.38% improvement in wear performance was detected compared to the unreinforced S-1 sample. Increasing reinforcement ratios had positive effects on the wear resistance of hybrid composites. Similarly, in the hardness study, an increase in hybrid reinforcements resulted in an increase in hardness. A similar situation in the hardness analysis supports the wear analysis. Furthermore, it can be shown that the volume losses rise in lockstep with the applied stress. Tirth [53] used the mixed casting approach to generate AA2218-Al<sub>2</sub>O<sub>3</sub> composites. The wear behavior of the produced composites under dry sliding conditions was investigated. In the wear analysis, it was reported that the volume loss increases with increasing load. It was also noted that the hardness resulting from the matrix reinforcement increases wear performance. Ambigai and Prabhu [38] produced hybrid nanocomposites by adding Si<sub>3</sub>N<sub>4</sub> to the Al-Gr matrix. They looked at the wear properties of the hybrid composites they created. They discovered that the wear rate of hybrid composites increased as the applied load increased. Furthermore, when

the stresses increased, the composite material was pressed further against the disc, increasing the wear rate.

SEM images taken from the worn surfaces of hybrid composites reinforced with SiC and BN reinforcements show that different wear mechanisms occur. Figure 10 shows the SEM photographs of the samples exposed to wear under a 5 N load. Oxidation wear and delamination are found to be the dominant wear mechanisms. Oxidation can be seen in materials due to the temperatures occurring during wear and the oxygen in the environment. During the wear test, stress foci may occur due to friction and loading. These foci can weaken the bond between the reinforcing fibers and the matrix material and cause cracks. These cracks can also cause delamination. In addition, when SEM images were carefully examined, it was determined that abrasive wear mechanisms were also seen. Especially in the S-1 sample, lines and grooves parallel to the slip direction draw attention. These scratches may occur due to the hardness of the opposite surface and the intervening of the pieces detached from the opposite surface. During wear, the surfaces of these grooves can expand and deepen to a certain extent. In addition, considering that there is only Al-Gr in the S-1 sample, it can be said that deep grooves are formed due to the



**Fig. 13** 3D surface topographies of hybrid composites under 5 N load

softness of the hybrid composite. It is thought that graphite forms a film layer on most wearing surfaces that facilitates contact between the disc surface and the material. This film layer also helps to reduce the coefficient of friction. It was reported that the rich graphite layer accumulated on the surfaces during wear increases the wear performance [54]. It was reported that ductile materials show better wear resistance at lower loads [55]. Nieto et al. [56] stated in their study on AMMC's that shallower grooves and higher hardness prevent abrasives from penetrating the composite surface.

Between the worn surface and the disc, there is a transition layer. This layer is also called the tribofilm surface. In addition to crumbled reinforcement particles and intermetallic particles on the tribofilm surfaces, iron oxide layers are also on the contact surfaces. By reducing contact between the counter surface and the composites, the hardness of this mechanically mixed layer can be maintained and deformation can be avoided [57]. In addition, the elements in the spectrum 1 region were determined by the EDS analysis performed on the S-5 sample (Fig. 11). As a result of the EDS analysis, both elements of the hybrid composite (C, N,

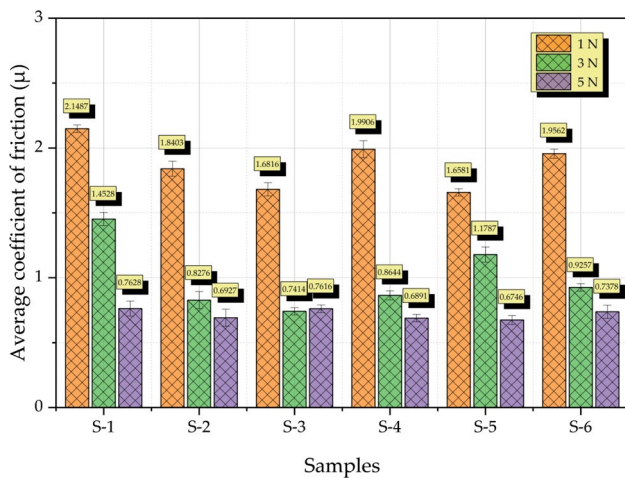


**Fig. 14** Average friction coefficient graph of hybrid composites subjected to wear under different loads

Al, Si) and elements of the opposite disc surface (V, Cr, Mn, Fe) were seen on the surface.

Figure 12 shows the EDS elemental mapping from the hybrid composite (S-6) and the weight ratios of the elements determined on the surface. A different color represents each detected element. The elements seen on the surface are respectively Al (74.374 wt.%), C (13.274 wt.%), Fe (6.715 wt.%), Si (3.988 wt.%), Cr (0.937 wt.%), N (0.501 wt.%), Mn (0.152 wt.%), V (0.059 wt.%). It was determined that the most abundant element on the surface was Al, the main matrix.

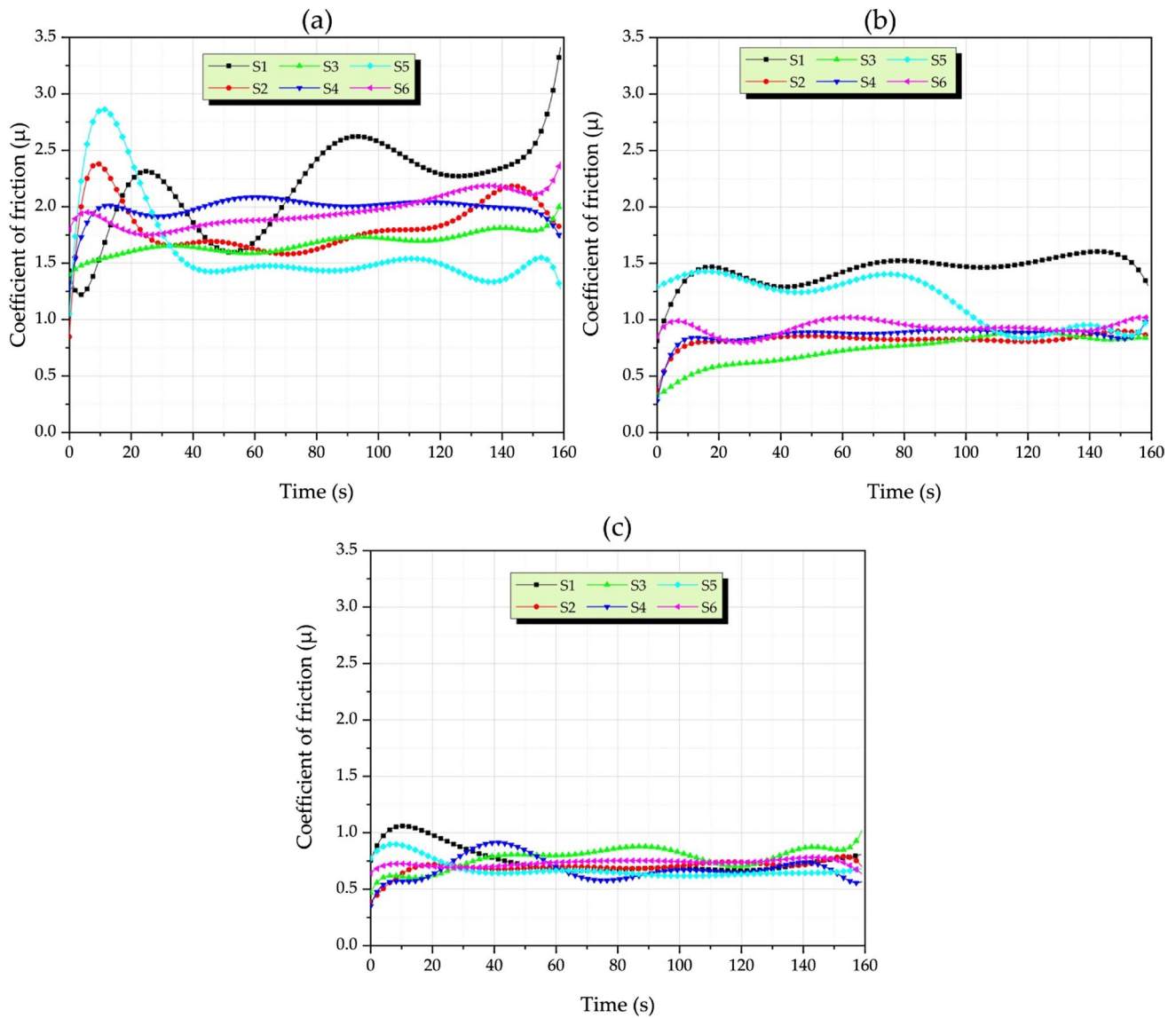
Figure 13 depicts 3D surface topographies of hybrid composites subjected to a 5 N load. It is seen that the surface is rougher in the S-2 sample compared to the S-1 sample. It can be said that the roughness of the S-3 sample is slightly reduced. It was observed that the surface roughness decreases with the increase in reinforcement ratio. This result was supported by the work implemented by Han and Nisar [58].

Figure 14 depicts the fluctuation of the average friction coefficients of hybrid composites under different loads. When the graph is viewed, the friction coefficients show a fluctuating variation. However, it is understood that the unreinforced S-1 sample has higher friction coefficients at all loads. In addition, it was determined that increasing loads decrease the friction coefficients. Ghosh et al. [59] examined the tribological characteristics of SiC reinforced AMMC and concluded that the friction coefficient of composite materials reduced as the applied load increased. Anand et al. [60] investigated the tribological performances of silicon carbide and porcelain doped Al6061 hybrid composites. They reported that the coefficients of friction decreased with increasing applied load. They also reported that this tendency is due to the hardening of the matrix material and the

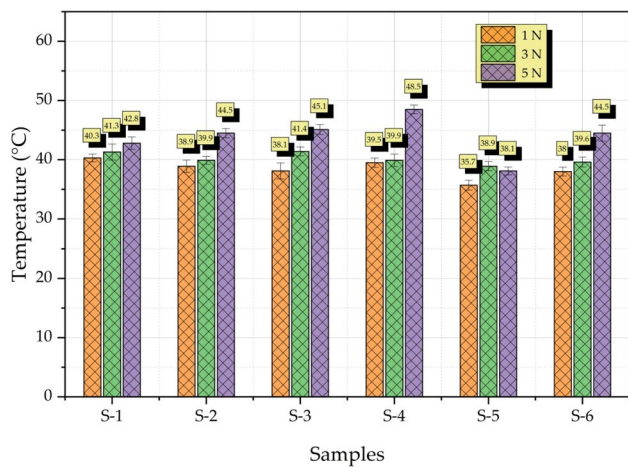
deformation of the asperities that occur with increasing load. With increasing loads, more particle fractures occur. Consequently, finer abrasive particulates are produced, which reduces the coefficient of friction. These abrasive particles, which are finer, form a film bed between the sample and the opposite surface and act as lubrication [61]. Reduction in friction coefficients of hybrid composites; was recorded as approximately 22.14% under 1 N load, about 48.96% under 3 N load, and about 11.56% under 5 N load.

Figure 15 depicts graphs depicting the temporal fluctuation of the friction coefficients of all hybrid composites under various loads. While a stable friction behavior was observed in Fig. 15b–c, an unstable friction behavior was detected in Fig. 15a. A thin friction film is formed on the material surface in the friction test performed under low load. For this reason, an unstable friction film may create and vary. Such a surface film structure can cause unstable frictional behavior. It can be seen that the friction coefficients of all samples drop as the applied loads rise. Therefore, plastic deformation may increase depending on the rise in the load between the hybrid composite and the counter surface. The increased plastic deformation is attributed to a decrease in the coefficient of friction. In addition, it can reduce friction by forming a film layer thanks to its Gr lubricant feature, which is found at a constant rate in hybrid composites. The lowest friction coefficient values were observed in the S-5 sample under 1 N load, in the S-3 sample under 3 N load, and in the S-5 sample under 5 N load.

Temperature increases occur due to friction between the material and the opposite disc surface. This process is quite complex. During the wear test, the heat caused by friction can cause thermal softening, welding and formations in the form of piles. These formations can be highly effective on wear performance. High temperatures in the wear zone decrease the specimen's hardness and cause the contact surfaces to expand [62]. Parameters such as reinforcement ratio, applied loads, wear distance and friction coefficient can cause different effects on temperature. Figure 16 represents the temperature graphs of hybrid composites measured under different loads. In general, increased load causes a rise in temperature. The lowest temperatures were determined as 35.7 °C under 1 N load, 38.9 °C under 3 N load and 38.1 °C under 5 N load. As a result of load increase, temperature increase can be seen in all samples. This might be due to the increasing penetration depth and strong abrasion effect of the particles breaking off on the sample surface as the load increases [63]. As a consequence of their wear studies on hybrid copper composites, Cheng et al. [64] found that temperatures grew in lockstep with applied stresses. They also observed that the samples applied with a load of 25 N had the greatest temperatures.



**Fig. 15** Time dependent changes of friction coefficients of all hybrid composites under different loads; **a** 1 N, **b** 3 N, **c** 5 N



**Fig. 16** Temperature graph of hybrid composites under different load conditions

### 4 Conclusions

In this study investigated the microstructure and tribological behaviors of hybrid composites produced based on SiC-BN reinforced Al-3Gr. The results are as follows:

- High relative density (96%) was obtained in composite materials by hot pressing.
- It was observed that the hardness increased with the increase in the type of reinforcement and the number of reinforcements. An improvement of approximately 49% was achieved compared to the single reinforced S1 composite.
- It was determined that as the reinforcement type and ratio increased, composite materials' volume loss decreased by approximately 80% in all load groups. Thus, it was

observed that the wear resistance of AMMCs with the highest reinforcement type and reinforcement ratio increased. Hardness analysis supports this opinion.

- As the applied load increases from 1 to 5 N, it was determined that the volume loss increases approximately two times, and the friction coefficient decreases about ten times. In sample no S-5 (5 N), the coefficient of friction was measured to be 0.6746.
- The friction coefficients in hybrid composites were shown to decrease with increasing applied load during wear. In sample no S-5, the coefficient of friction was measured to be 0.6746.
- Temperatures created during the wear test were shown to rise in lockstep with increasing load. Under 1 N load, the lowest wear temperature reported was 35.7 °C in sample S-5.
- Al-3Gr/SiC-BN hybrid composites exhibited better tribological performance and mechanical properties than Al-3Gr composite materials. Thus, these materials can be shown as suitable candidate materials for use in industry.

**Data availability** Sharing is not allowed as the data contained in this study is part of a work in progress.

## Declarations

**Conflict of interest** The author(s) stated that they had no possible conflicts of interest in relation to the research, writing, and/or publishing of this paper.

## References

- Gupta MK (2020) Analysis of tribological behavior of Al/Gr/MoS<sub>2</sub> surface composite fabricated by friction stir process. *Carbon Lett* 30(4):399–408
- Degirmenci U, Kirca M (2018) Design and mechanical characterization of a novel carbon-based hybrid foam: a molecular dynamics study. *Comput Mater Sci* 154:122–131
- Sap E (2020) Microstructural and mechanical properties of Cu-based Co-Mo-reinforced composites produced by the powder metallurgy method. *J Mater Eng Perform* 29(12):8461–8472
- Degirmenci U, Erturk AS, Yurtalan MB, Kirca M (2021) Tensile behavior of nanoporous polyethylene reinforced with carbon-based nanostructures. *Comput Mater Sci* 186:109971
- Kumar J, Singh D, Kalsi NS, Sharma S, Pruncu CI, Pimenov DY et al (2020) Comparative study on the mechanical, tribological, morphological and structural properties of vortex casting processed, Al-SiC-Cr hybrid metal matrix composites for high strength wear-resistant applications: fabrication and characterizations. *J Mater Res Technol* 9(6):13607–13615
- Şap S, Uzun M, Usca  A, Pimenov DY, Giasin K, Wojciechowski S (2021) Investigation on microstructure, mechanical, and tribological performance of Cu base hybrid composite materials. *J Mater Res Technol* 15:6990–7003
- Salur E, Aslan A, Kunto lu M, Acarer M (2021) Effect of ball milling time on the structural characteristics and mechanical properties of nano-sized Y<sub>2</sub>O<sub>3</sub> particle reinforced aluminum matrix composites produced by powder metallurgy route. *Adv Powder Technol* 32(10):3826–3844
- Mosleh-Shirazi S, Akhlaghi F, Li DY (2016) Effect of graphite content on the wear behavior of Al/2SiC/Gr hybrid nano-composites respectively in the ambient environment and an acidic solution. *Tribol Int* 103:620–628
- Sap E (2021) Microstructure and mechanical effects of Co-Ti powder particles on Cu matrix composites. *Russ J Non-ferrous Met* 62(1):107–118
- Zhou C, Zhou Y, Liu S, Zhang L, Song P, Zhang Q et al (2022) Lightweight and near-zero thermal expansion ZrW<sub>2</sub>O<sub>8</sub>-SiCnw/Al hybrid composites. *J Alloys Compd* 907:164444
- Li J, Li F, Wu S, L u S, Guo W, Yang X (2019) Variation of microstructure and mechanical properties of hybrid particulates reinforced Al-alloy matrix composites with ultrasonic treatment. *J Alloys Compd* 789:630–638
- Doğan K,  zɡ n M , S b tay H, Salur E, Eker Y, Kunto lu M et al (2022) Dispersion mechanism-induced variations in microstructural and mechanical behavior of CNT-reinforced aluminum nanocomposites. *Arch Civ Mech* 22(1):55
- Sharma A, Gupta G, Paul J (2021) A comprehensive review on the dispersion and survivability issues of carbon nanotubes in Al/CNT nanocomposites fabricated via friction stir processing. *Carbon Lett* 31(3):339–370
- Vani VV, Chak SKJMR (2018) The effect of process parameters in aluminum metal matrix composites with powder metallurgy. *Manuf Rev* 5:7
- Krishnan PK, Christy JV, Arunachalam R, Mourad A-HI, Muraliraja R, Al-Maharbi M et al (2019) Production of aluminum alloy-based metal matrix composites using scrap aluminum alloy and waste materials: Influence on microstructure and mechanical properties. *J Alloys Compd* 784:1047–1061
- Ashwath P, Joel J, Kumar HGP, Xavier MA, Goel A, Nigam T et al (2018) Processing and characterization of extruded 2024 series of aluminum alloy. *Mater Today: Proc* 5:12479–12483
- Chakrapani P, Suryakumari TSA (2021) Mechanical properties of aluminium metal matrix composites — a review. *Mater Today: Proc* 45:5960–5964
- Mistry JM, Gohil PP (2016) An overview of diversified reinforcement on aluminum metal matrix composites: tribological aspects. *Proc Inst Mech Eng J: J Eng Tribol* 231(3):399–421
- Iqbal A, Nuruzzaman DM (2016) Effect of the reinforcement on the mechanical properties of aluminium matrix composite: a review. *Int J Appl Eng Res* 11(21):10408–10413
- Sharma S, Singh J, Gupta MK, Mia M, Dwivedi SP, Saxena A et al (2021) Investigation on mechanical, tribological and microstructural properties of Al-Mg-Si-T6/SiC/muscovite-hybrid metal-matrix composites for high strength applications. *J Mater Res Technol* 12:1564–1581
- Mhaske MS, Shirsat UM (2021) An investigation of mechanical properties of aluminium based silicon carbide (AlSiC) metal matrix composite by different manufacturing methods. *Mater Today: Proc* 44:376–382
- Degirmenci  , Usca  A, Şap S (2023) Machining characterization and optimization under different cooling/lubrication conditions of Al-4Gr hybrid composites fabricated by vacuum sintering. *Vacuum* 208:111741
- Salur E, Acarer M, Şavkliyildiz   (2021) Improving mechanical properties of nano-sized TiC particle reinforced AA7075 Al alloy composites produced by ball milling and hot pressing. *Mater Today Commun* 27:102202
- Kumarasamy SP, Vijayananth K, Thankachan T, Pudhupalayam Muthukutti G (2017) Investigations on mechanical and



- machinability behavior of aluminum/flyash cenosphere/Gr hybrid composites processed through compocasting. *J Appl Res Technol* 15(5):430–441
25. Stojanovic B, Blagojevic J, Babic M, Velickovic S, Miladinovic S (2017) Optimization of hybrid aluminum composites wear using Taguchi method and artificial neural network. *Ind Lubr Tribol* 69(6):1005–1015
  26. Nagaraj N, Mahendra KV, Nagaral M (2018) Investigations on mechanical behaviour of micro graphite particulates reinforced Al-7Si alloy composites. *IOP Conf Ser: Mater Sci Eng* 310:012131
  27. Ul Haq MI, Anand A (2018) Dry sliding friction and wear behaviour of hybrid AA7075/Si3N4/Gr self lubricating composites. *Mater Res Express* 5(6):066544
  28. Miloradović N, Vujanac R, Stojanović B, Pavlović A (2021) Dry sliding wear behaviour of ZA27/SiC/Gr hybrid composites with Taguchi optimization. *Compos Struct* 264:113658
  29. Mosleh-Shirazi S, Akhlaghi F (2019) Tribological behavior of Al/SiC and Al/SiC/2 vol%Gr nanocomposites containing different amounts of nano SiC particles. *Mater Res Express* 6(6):065039
  30. Sharma P, Paliwal K, Dabra V, Sharma S, Sharma N, Singh G (2020) Influence of Silicon Carbide/Graphite addition on properties of AA6082 reinforced composites. *Aust J Mech Eng* 18(sup1):S176–S184
  31. Gowrishankar TP, Manjunatha LH, Sangmesh B (2020) Heat treatment and its effect on mechanical and wear properties of Al6061/Gr/TiC hybrid MMCs. *Int J Microstruct Mater Prop* 15(4):316–331
  32. Arivukkarasan S, Dhanalakshmi V, Stalin B, Ravichandran M (2018) Mechanical and tribological behaviour of tungsten carbide reinforced aluminum LM4 matrix composites. *Part Sci Technol* 36(8):967–973
  33. Balaji D, Vetrivel M, Ekambaram M (2021) Optimization of wear reduction on Al–TiO<sub>2</sub>–Gr powder metallurgy composites using D-optimal method. *Advances in Materials and Manufacturing Engineering: Select Proceedings of ICMME 2019*. Springer, Singapore
  34. Sharma P, Dabra V, Sharma S, Khanduja D, Sharma N, Sharma R et al (2019) Microstructure and properties of AA6082/(SiC + Graphite) hybrid composites. *Refract Ind Ceram* 59(5):471–477
  35. Senthil Kumar M, Vanmathi M, Sakthivel G (2021) SiC reinforcement in the synthesis and characterization of A356/Al<sub>2</sub>O<sub>3</sub>/SiC/Gr reinforced composite- paving a way for the next generation of aircraft applications. *SILICON* 13(8):2737–2744
  36. Danappa GT, Swamy RP (2019) Study on wear behaviour of Al7075 metal matrix composite with reinforced Gr and Nano TiO<sub>2</sub> particles by Taguchi method. *IOP Conf Ser: Mater Sci Eng* 577(1):012119
  37. Şap E (2021) Investigation of mechanical properties of Cu/Mo-SiCp composites produced with P/M, and their wear behaviour with the Taguchi method. *Ceram Int* 47(18):25910–25920
  38. Ambigai R, Prabhu S (2019) Fuzzy logic algorithm based optimization of the tribological behavior of Al-Gr-Si3N4 hybrid composite. *Measurement* 146:736–748
  39. Reddy PS, Kesavan R, Vijaya Ramnath B (2018) Investigation of mechanical properties of aluminium 6061-silicon carbide. *Boron Carbide Metal Matrix Compos Silicon* 10(2):495–502
  40. Usca ÜA, Şap S, Uzun M, Giasin K, Pimenov DY (2022) Evaluation of mechanical and tribological aspect of self-lubricating Cu-6Gr composites reinforced with SiC-WC hybrid particles. *Nanomater-Basel* 12(13):2154
  41. Singh JB, Cai W, Bellon P (2007) Dry sliding of Cu–15wt%Ni–8wt%Sn bronze: wear behaviour and microstructures. *Wear* 263(1):830–841
  42. Sap E, Uzun M (2022) A study of the microstructure and properties of copper composites reinforced with Co–Ti. *Met Sci Heat Treat* 63(9–10):558–563
  43. Liu Y, Chen Y, Deng J, Wang J (2021) N-doped aluminum-graphite (Al-Gr-N) composite for enhancing in-situ production and activation of hydrogen peroxide to treat landfill leachate. *Appl Catal B* 297:120407
  44. Liu Y, Tan N, Guo J, Wang J (2020) Catalytic activation of O<sub>2</sub> by AlO-CNTs-Cu<sub>2</sub>O composite for Fenton-like degradation of sulfamerazine antibiotic at wide pH range. *J Hazard Mater* 396:122751
  45. Ahmad SN, Hashim J, Ghazali MI (2005) The effects of porosity on mechanical properties of cast discontinuous reinforced metal-matrix composite. *J Compos Mater* 39(5):451–466
  46. Şenel MC, Gürbüz M, Koç E (2018) Fabrication and characterization of synergistic Al–SiC–GNPs hybrid composites. *Compos Part B-Eng* 154:1–9
  47. Tayeh T, Douin J, Jouannigot S, Zakhour M, Nakhli M, Silvain J-F et al (2014) Hardness and Young's modulus behavior of Al composites reinforced by nanometric TiB<sub>2</sub> elaborated by mechano-synthesis. *Mater Sci Eng A* 591:1–8
  48. Şenel MC, Gürbüz M, Koç E (2017) Fabrication and characterization of SiC and Si3N4 reinforced aluminum matrix composites. *Univers J Mater Sci* 5(4):95
  49. Firestein KL, Corthay S, Steinman AE, Matveev AT, Kovalskii AM, Sukhorukova IV et al (2017) High-strength aluminum-based composites reinforced with BN, AlB<sub>2</sub> and AlN particles fabricated via reactive spark plasma sintering of Al-BN powder mixtures. *Mater Sci Eng A* 681:1–9
  50. Idusuyi N, Olayinka JI (2019) Dry sliding wear characteristics of aluminum metal matrix composites: a brief overview. *J Mater Res Technol* 8(3):3338–3346
  51. Canakci A (2011) Microstructure and abrasive wear behaviour of B4C particle reinforced 2014 Al matrix composites. *J Mater Sci* 46(8):2805–2813
  52. Halil K, İsmail O, Sibel D, Ramazan Ç (2019) Wear and mechanical properties of Al6061/SiC/B4C hybrid composites produced with powder metallurgy. *J Mater Res Technol* 8(6):5348–5361
  53. Tirth V (2017) Dry sliding wear behavior of 2218 Al-alloy-Al<sub>2</sub>O<sub>3</sub>(TiO<sub>2</sub>) hybrid composites. *J Tribol.* <https://doi.org/10.1115/1.4037697>
  54. Akhlaghi F, Zare-Bidaki A (2009) Influence of graphite content on the dry sliding and oil impregnated sliding wear behavior of Al 2024-graphite composites produced by in situ powder metallurgy method. *Wear* 266(1):37–45
  55. Meshinchi Asl K, Masoudi A, Khomamizadeh F (2010) The effect of different rare earth elements content on microstructure, mechanical and wear behavior of Mg–Al–Zn alloy. *Mater Sci Eng A* 527(7):2027–2035
  56. Nieto A, Yang H, Jiang L, Schoenung JM (2017) Reinforcement size effects on the abrasive wear of boron carbide reinforced aluminum composites. *Wear* 390–391:228–235
  57. Riahi AR, Alpas AT (2001) The role of tribo-layers on the sliding wear behavior of graphitic aluminum matrix composites. *Wear* 251(1):1396–1407
  58. Khan MM, Nisar M (2022) Effect of in situ TiC reinforcement and applied load on the high-stress abrasive wear behaviour of zinc–aluminum alloy. *Wear* 488–489:204082
  59. Ghosh S, Sahoo P, Sutradhar G (2012) Wear behaviour of Al–SiCp metal matrix composites and optimization using Taguchi method and grey relational analysis. *JMMCE* 11(11):1085
  60. Anand VK, Aherwar A, Mia M, Elfakir O, Wang L (2020) Influence of silicon carbide and porcelain on tribological performance of Al6061 based hybrid composites. *Tribol Int* 151:106514
  61. Usca ÜA, Uzun M, Kuntoğlu M, Şap S, Giasin K, Pimenov DY (2021) Tribological aspects, optimization and analysis of

- Cu–B–CrC composites fabricated by powder metallurgy. *Materials* 14(15):4217
62. Subramanian C (2010) Wear properties of aluminium-based alloys. *Surface engineering of light alloys*. Woodhead publishing, London, pp 40–57
63. Prasad BK, Rathod S, Modi OP, Gupta GK, Yadav MS (2019) Two-body abrasive wear behaviour of in-situ Al-TiC particle composites: influence of TiC reinforcement and content in the alloy matrix and experimental parameters. *Tribol Finn J Tribol* 36(1–2):4–23
64. Cheng J, Mao M, Gan X, Lei Q, Li Z, Zhou K (2021) Microstructures, mechanical properties, and grease-lubricated sliding wear

behavior of Cu–15Ni–8Sn–0.8Nb alloy with high strength and toughness. *Friction* 9(5):1061–1076

**Publisher's Note** Springer Nature remains neutral with regard to jurisdictional claims in published maps and institutional affiliations.

Springer Nature or its licensor (e.g. a society or other partner) holds exclusive rights to this article under a publishing agreement with the author(s) or other rightsholder(s); author self-archiving of the accepted manuscript version of this article is solely governed by the terms of such publishing agreement and applicable law.